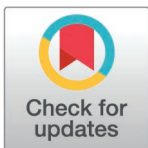SHORT REPORTS

Incomplete recombination suppression fuels extensive haplotype diversity in a butterfly colour pattern supergene

Rishi De-Kayne[1]*, Ian J. Gordon[2], Reinier F. Terblanche[3], Steve Collins[4],
Kennedy Saitoti Omufwoko[5], Dino J. Martins[6,7], Simon H. Martin[8]*

1 Department of Integrative Biology, University of California Berkeley, Berkeley, California, United States of America, 2 Centre of Excellence in Biodiversity and Natural Resource Management, University of Rwanda, Huye, Rwanda, 3 Department of Conservation Ecology & Entomology, University of Stellenbosch, Stellenbosch, South Africa, 4 African Butterfly Research Institute, Nairobi, Kenya, 5 Department of Ecology and Evolutionary Biology, Princeton University, Princeton, New Jersey, United States of America, 6 Turkana Basin Institute, Stony Brook University, Stony Brook, New York, United States of America, 7 Mpala Research Centre, Nanyuki, Kenya, 8 Institute of Ecology and Evolution, University of Edinburgh, Edinburgh, United Kingdom

* rdekayne@berkeley.edu (RD-K); simon.martin@ed.ac.uk (SHM)

Abstract

Supergenes can evolve when recombination-suppressing mechanisms like inversions promote co-inheritance of alleles at two or more polymorphic loci that affect a complex trait. Theory shows that such genetic architectures can be favoured under balancing selection or local adaptation in the face of gene flow, but they can also bring costs associated with reduced opportunities for recombination. These costs may in turn be offset by rare 'gene flux' between inverted and ancestral haplotypes, with a range of possible outcomes. We aimed to shed light on these processes by investigating the 'BC supergene', a large genomic region comprising multiple rearrangements associated with three distinct wing colour morphs in *Danaus chrysippus*, a butterfly known as the African monarch, African queen and plain tiger. Using whole-genome resequencing data from 174 individuals, we first confirm the effects of BC on wing colour pattern: background melanism is associated with SNPs in the promoter region of *yellow*, within an inverted subregion of the supergene, while forewing tip pattern is most likely associated with copy-number variation in a separate subregion of the supergene. We then show that haplotype diversity within the supergene is surprisingly extensive: there are at least six divergent haplotype groups that experience suppressed recombination with respect to each other. Despite high divergence between these haplotype groups, we identify an unexpectedly large number of natural recombinant haplotypes. Several of the inferred crossovers occurred between adjacent inversion 'modules', while others occurred within inversions. Furthermore, we show that new haplotype groups have arisen through recombination between two pre-existing ones. Specifically, an allele for dark colouration in the promoter of *yellow* has recombined into distinct haplotype backgrounds on at least two separate occasions. Overall, our findings paint a picture of dynamic evolution of supergene haplotypes, fuelled by incomplete recombination suppression.

Abbreviations: CNV, copy-number variable; GWAS, genome-wide association; IM, isolation-with-migration; LD, linkage disequilibrium; NAHR, non-allelic homologous recombination; PCA, principal components analysis.

Introduction

Genomic architectures that promote co-inheritance of certain combinations of alleles at multiple loci can be beneficial if they maintain adaptive allele combinations in the face of genetic mixing [1]. Such genetic architectures are referred to as supergenes, because they facilitate the inheritance of complex phenotypes in a simple Mendelian fashion, (reviewed in [2]). Supergenes are often associated with chromosomal inversions, which have the unique feature of reducing recombination between haplotypes with distinct inversion orientations while allowing free recombination between haplotypes with the same orientation. This effectively divides the population into two subpopulations over a defined portion of the genome [3]. Supergenes have been found to underpin trait polymorphisms under balancing selection, such as alternative life-history and reproductive strategies [4–8] and mimetic colouration [9]. Inversions can also be favoured during local adaptation in the face of gene flow between two distinct environments if they maintain locally adapted combinations that differentiate ecotypes [10–12]. Here, we include these cases of locally adapted inversions under the umbrella term 'supergenes', provided they still act to maintain allele combinations that would otherwise be broken down through gene flow and recombination. Genomic studies of species that exhibit local adaptation frequently uncover inversions underpinning differences between ecotypes [13–16], and 'bottom-up' analyses have identified signatures consistent with locally adapted inversions even when the specific traits they may be associated with are unknown [17–19]. This suggests that supergene architectures may be ubiquitous in nature, highlighting a need to better understand their evolutionary dynamics.

Recent theoretical and empirical work suggests that supergenes may evolve over time in their structure, composition, and effects on phenotype and/or fitness. First, supergene structure can evolve through recurrent chromosomal rearrangements. Studies across multiple systems show that supergenes often comprise several rearrangements, implying stepwise growth in the region of suppressed recombination (e.g., in *Heliconius* butterflies [20], *Danaus* butterflies [21], and *Solenopsis* fire ants [6]). In addition to allowing the incorporation of additional co-adapted alleles at other loci, subsequent rearrangements of the supergene region can cause recombination suppression between more than two distinct haplotypes [21]. Second, even without physical expansion, the repertoire of traits affected by an inversion supergene may expand over time as additional alleles become established at other loci within the region of recombination suppression [11,17]. The fitness consequences of a supergene could also change if selective pressures change over time or across space, potentially limiting the value of a supergene in a changing environment or during dispersal into a new environment [22]. Even in a stable environment, inversion supergenes may be subject to accumulation of increased mutational load compared to the rest of the genome due to their reduced opportunities for recombination and reduced effective population size (N_e) (due to the effective subdivision of the population in that part of the genome) [23–25]. Some theoretical models suggest that this may lead to heterokaryotype advantage through sheltering of recessive deleterious mutations (associative overdominance) [23–25], or failure of locally adapted inversions to reach high frequency [26].

Another process that contributes to the evolution of inversion supergenes is rare recombination in heterokaryotypes, which results in some degree of gene flux between haplotypes. While single crossovers within inversions are usually strongly suppressed due to the production of unbalanced chromosomes [27], large inversions may allow for double crossovers [28], which result in the exchange of genetic material between arrangements, effectively creating a mosaic haplotype. In addition, gene flux of short fragments can occur through non-crossover gene conversion. This has been shown experimentally in *Drosophila* to occur at least as often within inversion heterokaryotypes as in syntenic regions [28–33]. Indirect

inference in natural populations of a range of different species support the existence of considerable gene flux within inversions [32,34–40], and suggest that a drift-flux equilibrium can be reached [3]. Gene flux reduces linkage disequilibrium (LD) within inversions [41] and provides a means by which they may avoid some of the costs of recombination suppression described above, potentially facilitating their long-term persistence [6,23,37]. In some supergenes, sequence divergence suggests persistence of polymorphism for millions of years, even through multiple speciation events [21,37]. However, the role of gene flux in supergene temporal dynamics remains under-explored. A compelling example of recombination creating a novel haplotype associated with a distinct phenotypic class is seen in the supergene that controls reproductive morphology and behaviour in the ruff [5,37]. On the other hand, a mimicry supergene in *Papilio* butterflies shows phylogenetic relationships consistent with wholesale 'allelic turnover', in which new haplotypes arise (possibly via recombination) and replace ancestral ones [42]. Case studies such as these provide valuable insights into the range of processes contributing to supergene evolution.

Danaus chrysippus, a butterfly known as the African monarch, African queen, and plain tiger, presents an opportunity to investigate the contributions of the above processes to the evolution of a large, ancient supergene. Like other milkweed butterflies, *D. chrysippus* has bright warning patterns that advertise its toxicity. Across its range, it is divided into several parapatric morphs with distinct warning patterns that meet in a broad hybrid zone in eastern central Africa (Fig 1A) [43,44]. Phenotypic differences in two forewing traits are controlled by the 'BC supergene' on chromosome 15, which links at least two colour patterning loci that were originally described in crossing experiments: The 'B' locus affects whether background colour is dark/brown (dominant *B* allele) or pale/orange (recessive *b* allele) and the 'C' locus determines whether the apical black tip and white band is present (recessive *c* allele), or absent (dominant *C* allele) [21,45–48]. Previous genomic comparisons of a limited number of populations revealed the existence of three divergent haplotype groups (also called 'alleles') at the BC supergene, which were named according to the morphs in which they are found: 'orientis' (*Bc*, Southern Africa), 'klugii' (*bC*, East Africa), and 'chrysippus' (*bc*, West Africa, North Africa, Mediterranean, Asia) [45]. Note that while a distinct morph 'alcippus' is found in West Africa, it is defined by its hindwing phenotype, controlled by a locus on a different chromosome, but carries the chrysippus haplotype at the BC supergene. Chromosome-scale assemblies of each of the three haplotypes revealed that, rather than comprising a single large inversion, the BC supergene is underpinned by a complex, modular rearrangement including several inversions and a large copy-number variable (CNV) region [21]. This complex architecture helps to explain how recombination is suppressed between more than two divergent haplotype groups. Phylogenetic analysis showed that the rearrangements probably occurred in a stepwise manner, beginning several million years ago, and that the supergene has persisted through multiple speciation events [21]. Intriguingly, an additional rearrangement has recently occurred and risen to high frequency in a small region of East Africa: a fusion of chr15 to the female-specific W chromosome [45,49]. Because crossing-over is limited to males in Lepidoptera, this fusion represents an additional mechanism of recombination suppression, effectively creating a new female-specific sub-group of the chrysippus haplotype [45]. There is also evidence for rare recombination within the supergene based on phenotypes in crossing experiments, and a putative recombinant haplotype assembly from a hybrid-zone individual [21,50]. Taken together, the above findings suggest that, despite its age, the BC supergene continues to evolve, raising questions about the full extent of diversity at this locus and the role of recombination in shaping this diversity.

Here, we investigate haplotype diversity and evolution of the BC supergene using genomic data from 174 *D. chrysippus* individuals representing 14 regions across Africa and southern
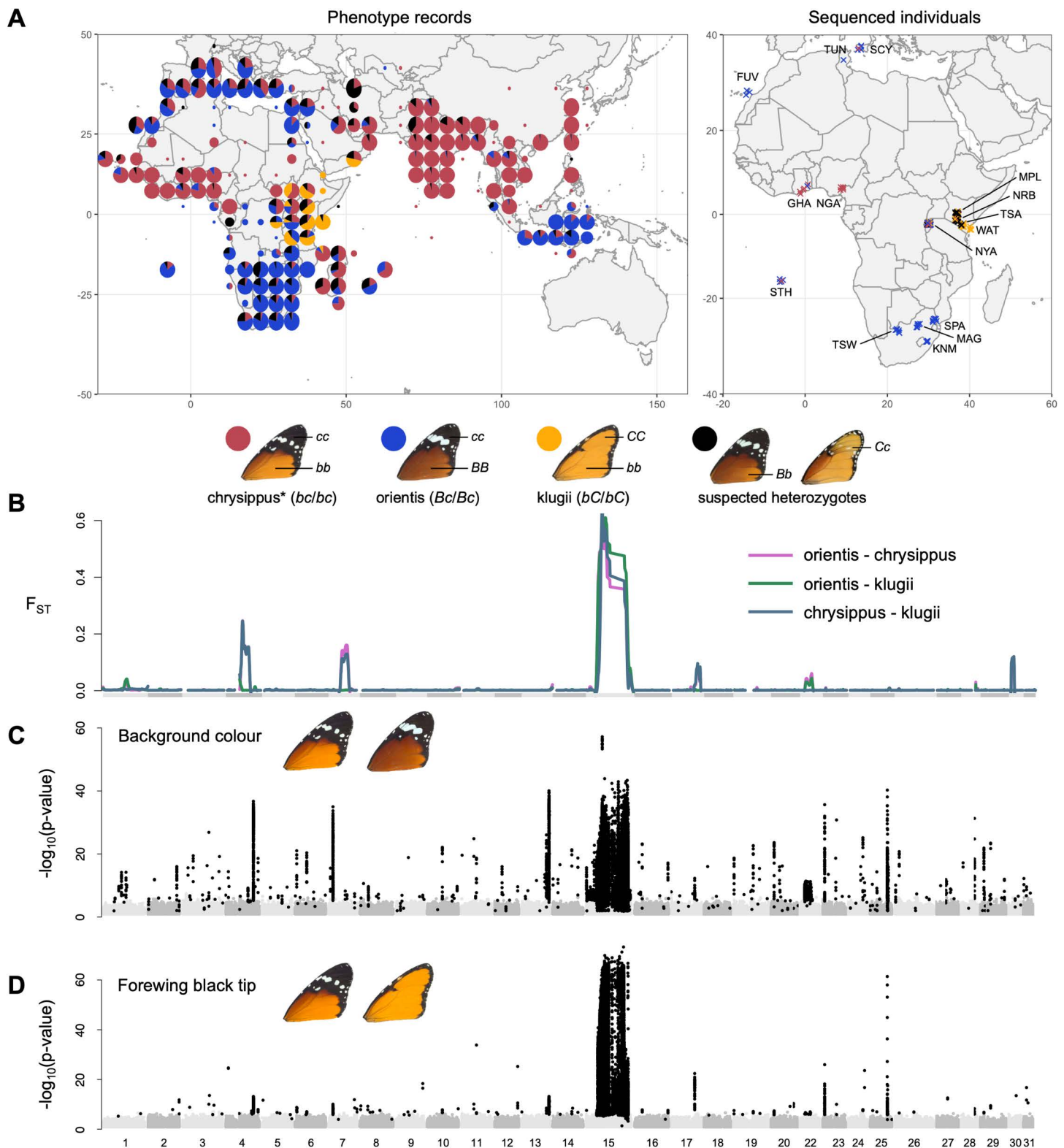
Fig 1. Broad geographic distribution of *Danaus chrysippus* morphs and our continent-wide sampling of individuals spans wing pattern variation that is underpinned largely by variation on chromosome 15. (**A**) Geographic distribution of the three main *D. chrysippus* forewing morphs; chrysippus, orientis, and klugii as well as putative heterozygotes (data from manual curation of GBIF record and other scientific collections, following the approach in [44]; left) and sampled locations of *D. chrysippus* individuals used for genomic analysis in the present study (right). Public domain map from naturalearthdata.com. Morphs and their corresponding inferred

genotypes at the B and C loci are shown below. Note that for our purposes the forewing morph 'chrysippus' includes the west-African morph 'alcippus', which has the same forewing phenotype, but differs in its hindwing phenotype. (**B**) Genome-wide patterns of F_{ST} between morphs (smoothed across discrete 50 kb windows) highlighting significant differentiation along the length of the chr15 supergene region. (**C, D**) Genome-wide associations between SNP variation and (**C**) background colouration (individuals were scored as light, intermediate, or dark; $N = 172$, following [44]) and (**D**) forewing band presence/absence (individuals were scored as absent, partial, or present; $N = 172$, following [44]) reflecting significant associations between this region and wing-pattern variation. Significant associations, as identified via permutation tests ($p < 0.05$), are represented by black points. The data underlying this figure can be found in https://doi.org/10.5281/zenodo.14718778 and S1 Table.

https://doi.org/10.1371/journal.pbio.3003043.g001

Europe. We first confirmed that the supergene links loci controlling two distinct wing colour pattern traits. We then describe haplotype diversity and identify additional divergent haplotype groups beyond those previously described. Comparable levels of genetic diversity in each haplotype group and across most of the discrete structural modules of the supergene argues against ongoing allelic turnover, and instead suggest a long-term polymorphism, probably driven by local adaptation. Perhaps most intriguingly, we find abundant evidence of recombination and gene flux between haplotype groups, with crossovers having occurred both between adjacent inversions and within individual inversions, leading to exchange of functional colour pattern alleles. These results support a role for somewhat rare recombination in the diversification and long-term persistence of supergene haplotypes.

Results

Widespread sampling confirms that the BC supergene is associated with forewing colour variation and is the main axis of genetic variation

We analysed resequenced genomes of 174 individual butterflies spanning the three core *D. chrysippus* forewing morphs, 'chrysippus' (note that for our purposes, this also includes form 'alcippus', which differs primarily in its hindwing), 'orientis', and 'klugii', as well as intermediate morphs (Fig 1A and S1 Table). Our sampling includes areas of monomorphism for each morph: western Africa, South Africa, and southeastern Kenya, respectively. We also sampled the hybrid zone (sampled in Rwanda and central Kenya, where all three forewing morphs and intermediates are found), and North Africa and the Mediterranean (where two of the three morphs, and intermediates are found). Twelve sequenced individuals were bred in captivity from parents of mixed or unknown origins and were not assigned to any geographic group. Pairwise F_{ST} between three monomorphic locations in South Africa (TSW population, orientis morph), Nigeria (NGA population, chrysippus morph) and Eastern Kenya (WAT population, klugii morph), is close to zero genome-wide, with the exception of a few large peaks, including the largest on chromosome 15 (chr15), as described previously (Fig 1B and S1 Table) [45]. Genome-wide principal components analysis (PCA) for all autosomes excluding chr15 further supports minimal genetic structure outside of the BC supergene, except that samples from the small island of St. Helena, as well as captive-bred families each cluster separately from the remaining wild individuals (Fig A in S1 Text).

Genome-wide association (GWAS) analysis confirms that the BC supergene region on chr15 is associated with two forewing traits: pale/dark background wing colour (also known as the B locus; Fig 1C), and the presence/absence of the forewing black tip and white band (also known as the C locus; Fig 1D). In addition to a large peak of association in the supergene, there are several peaks of association with pale/dark variation on other chromosomes, suggesting that other loci also contribute to this trait. A repeat of the GWAS using only samples from the hybrid zone (NYA, NRB, MPL populations, $N = 87$) recapitulates the same general result (Fig B in S1 Text), confirming that the observed associations are not driven by correlated selection on other traits that follow a similar geographic distribution. The cluster of SNPs most strongly associated with background wing colour fall between two genes: *yellow*,

which is known to be involved in melanin synthesis and colouration in other insects [51], and the *achaete-scute complex protein T3-like*, which has been shown to be involved in wing scale development across Lepidoptera [52]. The SNPs most strongly associated with the presence or absence of the forewing black tip were found to fall within the CNV region of the supergene (Fig C in S1 Text). These findings suggest that the B and C loci are distinct, and that the supergene is favoured because it maintains locally adapted combinations of alleles at these loci, and probably others among the ~ 150 genes it encompasses, in the face of gene flow.

Extensive genetic variation at the BC supergene

We previously described three divergent haplotype groups (sometimes called 'alleles') of the BC supergene, corresponding to the three forewing morphs, maintained by several inversions, intra-chromosomal translocations, and copy-number differences that suppress recombination [21,45]. We therefore expected that diploid genotypes across the BC supergene would form six distinct genetic clusters corresponding to the three homozygous and three heterozygous states. However, as we describe below, several lines of evidence suggest that there are additional divergent haplotypes, and possible recombinants. First, both a distance-based Neighbor-Net network and PCA for the complete supergene (excluding the CNV region) show more complex genetic structuring than we expected (Fig 2A and Fig A in S1 Text). Three clusters representing homozygous genotypes for the three previously described haplotype groups are identifiable (Fig 2A), and include individuals previously matched to these genotypes [21]. One large cluster of individuals is intermediate between the known chrysippus and klugii homozygotes (Fig 2A) and includes known heterozygotes between chrysippus and klugii from crosses and suspected wild heterozygotes based on wing patterns. However, numerous other individuals are dispersed across the network at varying distances between the three homozygous clusters. We therefore hypothesised that in addition to heterozygotes among the three known haplotype groups, our sampling may include additional divergent haplotype groups and/or recombinants among the three common haplotypes.

Given the complex relationships observed, we attempted to naively identify distinct haplotype groups using Admixture [53] analysis, in which each individual is modelled in terms of its ancestry components from k source populations. Because recombination should occur freely among haplotypes with the same structural arrangement, and should only be suppressed among those with different arrangements, the supergene region should comprise a set of semi-isolated sub-populations. We predicted that "heterozygous" individuals (i.e., carrying two divergent haplotypes) will appear as admixed, with approximately 50% ancestry contributions from two source populations, while homozygotes should be assigned 100% ancestry from a single source. All models with $k = 3$ (matching our *a priori* hypothesis) and above captured the three previously described haplotype groups corresponding to the klugii, chrysippus, and orientis morphs. These are represented in clusters of homozygous (100% ancestry) individuals from eastern, western, and southern Africa, respectively, while most hybrid-zone individuals appear heterozygous, with 50% ancestry proportions (Figs E–H in S1 Text). However, as described below, the models with $k = 4$– 6, which all have lower cross-validation error than $k = 3$ (Fig D in S1 Text), provide compelling evidence for the existence of additional divergent haplotype groups that had not been previously described.

We have chosen to present the ancestry assignments according to the model with $k = 4$ sources in Fig 2 (see pie charts in Fig 2A and 2B), because our sampling included homozygotes for all four putative haplotype groups. The fourth source population is inferred to contribute ~ 100% ancestry to two South African individuals, and ~ 50% ancestry to several others. We therefore infer that a fourth arrangement of the supergene occurs in southeast Africa. This haplotype group is cryptic in the sense that it is associated with a forewing
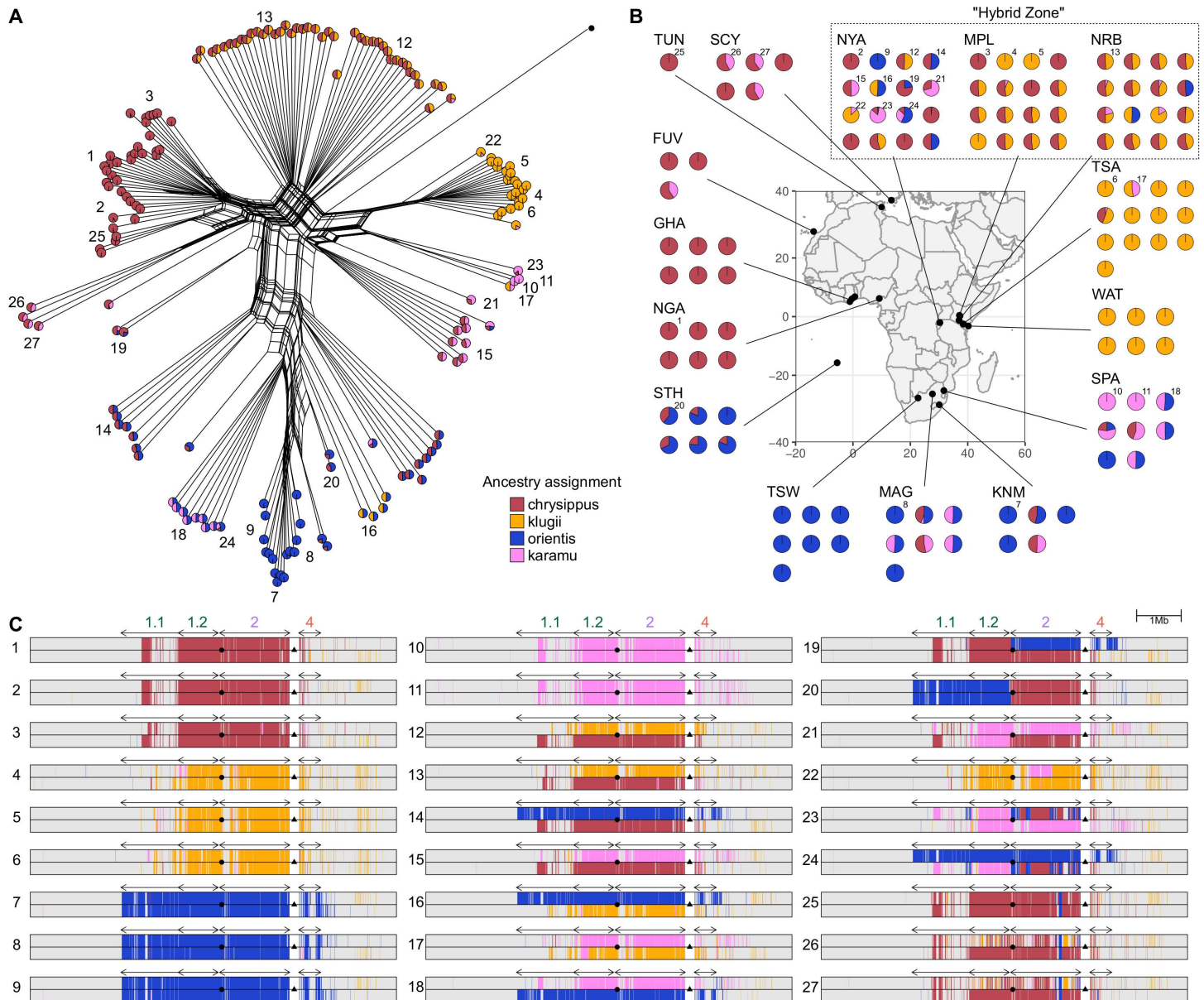
Fig 2. Genetic clustering and ancestry painting suggest additional divergent haplotype groups, and recombinants. (**A**) Neighbor-Net network for unphased diploid genotypes across the BC supergene (excluding the copy-number variable [CNV] region). Each tip represents one diploid individual, and the network is constructed based on average pairwise genetic distances considering both haplotypes in each individual. We therefore expect 'heterozygous' individuals carrying two distinct haplotypes to be at intermediate positions in the network. Numbers indicate the 27 representative individuals for which ancestry painting is shown in panel C. The single individual represented by a black dot is the *Danaus melanippus* outgroup. (**B**) Localities for sequenced individuals (public domain map from naturalearthdata.com). Pie charts in panels A and B represent inferred ancestry components for each diploid individual from Admixture analysis with k = 4 source populations (See Figs D–H in S1 Text for plots with other values of k). Note that for highly sampled localities, an arbitrary subset of sequenced individuals is shown in panel B. Numbered individuals correspond with those in Panels A and C. **C.** Ancestry painting across the central portion of chr15 including the BC supergene for 27 representative individuals, including homozygotes, heterozygotes and putative recombinants. See Figs I and J in S1 Text for ancestry painting for all individuals. The CNV region is excluded from the plot for convenience as it cannot be reliably genotyped (represented as a white gap). Arrows above the plots indicate the locations of inverted tracts 1.1 (1.3 Mb). 1.2 (0.9 Mb), 2 (1.6 Mb) and 4 (0.5 Mb). The inferred location of the B locus (*yellow*) is indicated by a circle in the centre of each plot. The approximate location of the C locus is indicated by a triangle in the gap where the copy-number variable region is found. The data underlying this figure can be found in https://doi.org/10.5281/zenodo.14718778.

https://doi.org/10.1371/journal.pbio.3003043.g002

phenotype indistinguishable from that of orientis. Hereafter, we refer to this as the 'karamu' haplotype group.

In the model with $k = 5$ sources (Fig G in S1 Text), the fifth cluster captures the previously described neo-W fusion—a lineage of chr15 haplotypes that arose recently in East Africa when a copy of chr15 from the chrysippus haplotype group fused to the female-limited W sex chromosome [45,49]. These females are each assigned ~50% ancestry from this source, consistent with W being haploid in females. We previously showed that the neo-W-chr15 fusion occurred recently and spread to high frequency in southern Kenya over the past 2,200 years [45]. The high sequence similarity and complete lack of recombination of the neo-W explains how it is identifiable as a distinct genetic cluster despite its recent separation from the standard chrysippus haplotype group.

In the model with $k = 6$ sources (Fig H in S1 Text), several individuals from North Africa and the Mediterranean are assigned to a sixth distinct cluster, suggesting yet another divergent haplotype group. We hypothesise that, similar to the karamu haplotype from southeast Africa, another distinct arrangement of chr15 likely occurs north of the Sahara. However, subsequent analyses (described below) suggest that none of our sequenced individuals are homozygous for this haplotype, limiting our ability to further investigate its status.

Ancestry painting confirms additional haplotype groups, as well as recombinants

To investigate fine-scale haplotype ancestry and recombination across the BC supergene region, we applied two ancestry-painting methods. These aim to assign ancestry for phased-inferred haplotypes based on pre-defined source populations, using either a hidden Markov model [54] or defined windows of SNPs (see Methods for details). We used populations WAT, TSA, and NGA as reference sets representing the klugii, orientis, and chrysippus haplotype groups, due to their monomorphic clustering (Fig 2B). In addition, we used the two individuals from the SPA population showing 100% karamu ancestry to represent this fourth haplotype group (Fig 2B). Both ancestry-painting methods agree strongly with our inferences from the Admixture analysis. All four haplotype groups occur as intact haplotypes in most individuals, with large numbers of both homozygotes (individuals 1–11 in Fig 2C) and heterozygotes (individuals 12–18 in Fig 2C). See Figs I and J in S1 Text for all individuals. Heterozygotes are particularly common in the hybrid-zone (populations NYA, MPL, and NRB in Rwanda and central Kenya, Figs I and J in S1 Text).

Ancestry painting also identifies individuals with mosaic ancestry consistent with recombination between the divergent haplotypes. Most of these putative recombinant haplotypes appear to be simple chimeras that result from a single crossover located between two adjacent inversions (see for example individuals 19–21 in Fig 2C). However, there are also instances of more fine-scale mosaic ancestry consistent with recombination within inversions (see for example individuals 22–25 in Fig 2C). While gene conversion can lead to the transfer of small haplotype tracts within inversions (tract lengths vary across taxa, but estimates suggest they are typically <4 kbp in length; [55]), this process cannot explain the scale of mosaic ancestry tracts we observe (tens to hundreds of kb). Instead, these patterns are more consistent with occasional double crossovers, which allow genetic exchange within the inversions without the formation of unbalanced gametes (but see Discussion). Some of these recombinant haplotype patterns appear multiple times in unrelated individuals, implying that they may be increasing in frequency in the population (see for example individuals 23–24 in Fig 2C). Unsurprisingly, most recombinant haplotypes are found in the hybrid zone (Figs I and J in S1 Text). However, we were surprised to find two distinct recombinant haplotypes present in the genomes from

the small island of St. Helena (STH population), where only one of the six sequenced individuals did not carry a recombinant haplotype (Figs I and J in S1 Text).

Ancestry painting failed to assign ancestry to one of the haplotypes in some individuals from North Africa and the Mediterranean (see for example individuals 26–27 in Fig 2C). These are individuals that were assigned to the sixth cluster in the admixture analysis with $k = 6$ sources (Fig H in S1 Text). This supports the existence of an additional divergent haplotype of the BC supergene that occurs north of the Sahara. Other members of this population carry a chrysippus-like haplotype, with some evidence for recombination with orientis (seen in individuals 25–27 in Fig 2C). Because no individual is homozygous for the additional divergent haplotype, we were unable to include it as a source for ancestry painting, and it was not included in our subsequent analyses.

In summary, our findings suggest that there are (at least) six divergent haplotype groups of the BC supergene that experience suppressed recombination with respect to each other. Three were previously assembled and found to have distinct arrangements (chrysippus, klugii, and orientis); one results from fusion of chr15 to the W chromosome (neo-W-chrysippus); and two are newly identified here based on genetic clustering, but probably also represent distinct structural arrangements (karamu and the unnamed haplotype from North Africa and the Mediterranean) (Table 1).

Diversity and divergence patterns are consistent with long-term polymorphism

One possible explanation for the coexistence of multiple haplotypes associated with the same wing phenotype in the same population (e.g., karamu and orientis haplotypes in the SPA population) is that we are witnessing an ongoing 'allelic turnover' event [42], in which a new haplotype is replacing an older one. If a new haplotype arose through a novel structural rearrangement, it is expected to have undergone a bottleneck of $N = 1$ at its conception [3], which would result in dramatically reduced diversity immediately following its origin. Older haplotypes should have had the opportunity to recover diversity following their initial bottleneck, but are nevertheless still expected to have lower diversity than the genomic background level because inversions effectively divide the species into sub-populations with lower effective population size across the inverted region (even for the ancestral orientation) [3]. We therefore expected that all haplotype groups may show reduced within-group diversity within the inverted regions, but we hypothesised that a more pronounced reduction may be observed in those with derived inversion orientations: orientis and chrysippus [21] and possibly the newly identified karamu haplotype. Consistent with expectations, diversity is lower within the inverted regions of chr15 compared to collinear regions in all four haplotype groups (Fig 3B).

Table 1. Six divergent haplotype groups of the BC supergene.

Haplotype Name	Geographic region(s)	Background colour (B locus allele)	Forewing tip and band (C locus allele)	Conventional name of morph
chrysippus	West Africa, North Africa and Mediterranean, Asia	Pale (b)	Present (c)	chrysippus, alcippus
klugii	East Africa	Pale (b)	Absent (C)	klugii
orientis	Southern Africa	Dark (B)	Present (c)	orientis
karamu	Southeast Africa	Dark (B)	Present (c)	orientis
neo-W-chrysippus	East Africa (Hybrid Zone)	Pale (b)	Present (c)	N/A (never homozygous)
Unnamed	North Africa and Mediterranean	Unknown (no homozygotes)	Unknown (no homozygotes)	Unknown (no homozygotes)

https://doi.org/10.1371/journal.pbio.3003043.t001

The extent of diversity reduction is notably similar in the four groups, with the exception that orientis has lower diversity in inverted region 1.1, which is known to be uniquely inverted in orientis. No haplotype group has diversity approaching zero, as would be expected under rapid, recent allelic turnover, so these patterns are more consistent with a long-term polymorphism at the BC supergene.

Genetic divergence and differentiation between haplotype groups are also consistent with relatively ancient origins. Elevated F_{ST} and net divergence (d_a) are restricted to the rearranged parts of the chromosome ([Fig 3](#)), consistent with recombination suppression being restricted
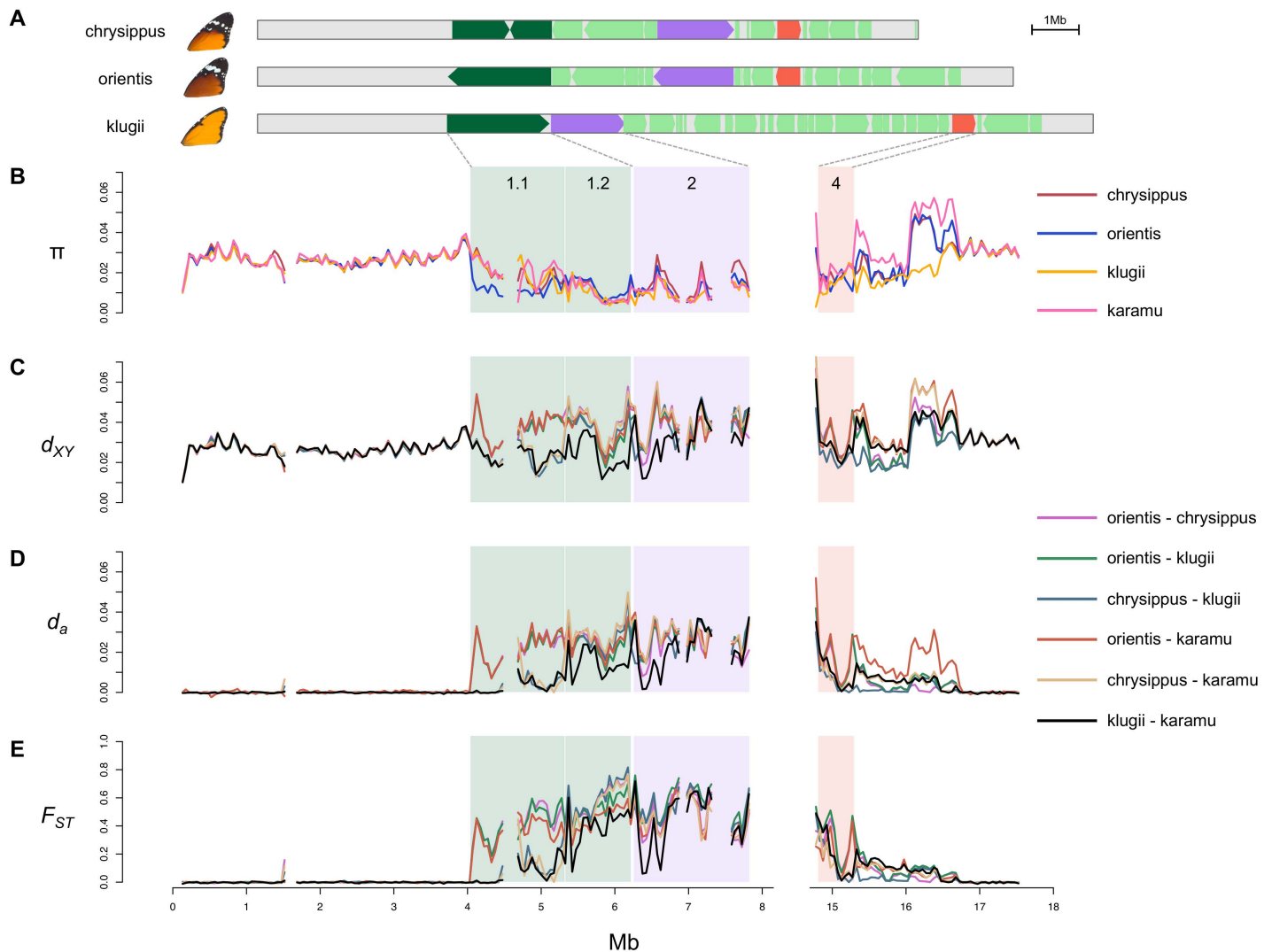

Fig 3. The supergene region has reduced genetic diversity in all haplotype groups and elevated genetic differentiation between them, but no evidence for a very recent origin of any haplotype. (**A**) A graphical representation of the structural variation across the chrysippus, orientis, and klugii haplotypes described in [21]. The additional divergent haplotypes described in the present study have not yet been assembled with long reads, so their structures remain unknown. The three previously assembled haplotypes evolved through rearrangements of four main regions (indicated with different colours; arrows indicate orientation relative to the ancestral state). Regions 1.1, 1.2, 2, and 4 remain in single copy and can be reliably aligned and genotyped. (**B–E**) Population summary statistics computed in non-overlapping 50 kb windows for representative populations of chrysippus (NGA population), orientis (TSW), klugii (WAT), and karamu (two homozygous individuals from the SPA), plotted across chr15 (excluding the copy-number variable region). Note that the reference genome is from a klugii haplotype, hence regions 1 and 2 are adjacent. Statistics plotted are: (B) nucleotide diversity (π), (C) absolute pairwise divergence (d_{XY}), (D) net pairwise divergence (d_a), and (E) pairwise differentiation (F_{ST}). The data underlying this figure can be found in https://doi.org/10.5281/zenodo.14718778.

https://doi.org/10.1371/journal.pbio.3003043.g003

to the supergene (note that regions 1.1 and 4 are only inverted in orientis and are collinear in klugii and chrysippus). Similar levels of differentiation are seen between these three previously described haplotype groups across most of the supergene (excluding region 1.1), which may indicate that the arrangements all occurred around the same time, although this pattern would also be expected under mutation-drift-flux equilibrium [3]. However, divergence and differentiation are both notably lower between klugii and the newly described karamu haplotype group across most of the supergene, consistent with either a more recent divergence between these haplotypes, or a higher rate of gene flux between them. This is intriguing, because these haplotypes are associated with distinct wing phenotypes. This raises the possibility that gene flux between haplotype groups has allowed the exchange of functional alleles.

Recombination between supergene haplotypes has exchanged wing colour alleles

We set out to test whether the evolution of the karamu haplotype may have arisen through recombination between haplotype groups. Specifically, we applied topology weighting [56] using TWISST2 to ask whether there are tracts in which karamu is more closely related to orientis than to klugii. This revealed that karamu clusters broadly with klugii throughout the length of the supergene, but there are multiple narrow tracts at which it clusters more closely with orientis, particularly in inverted region 2 (Fig 4A). Ancestry painting using Loter [54] confirms that one such narrow tract is a 20 kb region containing the gene *yellow* and part of its promoter, including nine of the 10 SNPs most strongly associated with wing background colouration according to our GWAS (Fig 4B). This therefore suggests that incorporation of the orientis-like allele at *yellow* (i.e., the *B* allele at the B locus) through recombination causes the karamu haplotype to produce a dark wing colour phenotype matching that of orientis, despite otherwise being more klugii-like in its overall ancestry. We hypothesise that a similar allelic exchange at the C locus causes karamu individuals to share the forewing black tip phenotype of orientis, but we are unable to test this hypothesis, as this trait maps to the CNV region in which genotyping and ancestry assignment are unreliable.

We identified a second probable case of recombination affecting background colouration. Several individuals from North Africa and the Mediterranean are homozygous for chrysippus-like haplotypes according to chromosome painting (see for example individual 25 in Fig 2C), but have dark background colouration similar to that seen in orientis. We again tested for fine-scale mosaic ancestry in two of these individuals using topology weighting and ancestry painting. A very similar pattern to the karamu case is observed: these individuals cluster strongly with chrysippus throughout the supergene, but carry narrow orientis-like tracts (Fig 4C), including a 10 kb tract in the promoter region of *yellow* encompassing all 10 SNPs most strongly associated with dark background colouration (Fig 4D). This represents a distinct event in which orientis-like alleles (i.e., the *B* allele at the B locus) have been incorporated into a different genetic background through recombination within an inversion, leading to an altered phenotype.

Historial gene flux also occurred between the major supergene haplotypes

Based on the extensive evidence for recombination observed, we hypothesised that even the three originally described haplotype groups (orientis, klugii, and chrysippus) may have been historically shaped by gene flux. To explore this possibility, we first ran another topology weighting analysis to examine fine-scale relationships between these three groups. This generally agrees with the supergene structure: in each rearrangement, the predominant genealogy clusters groups according to whether they carry the rearranged or ancestral arrangement
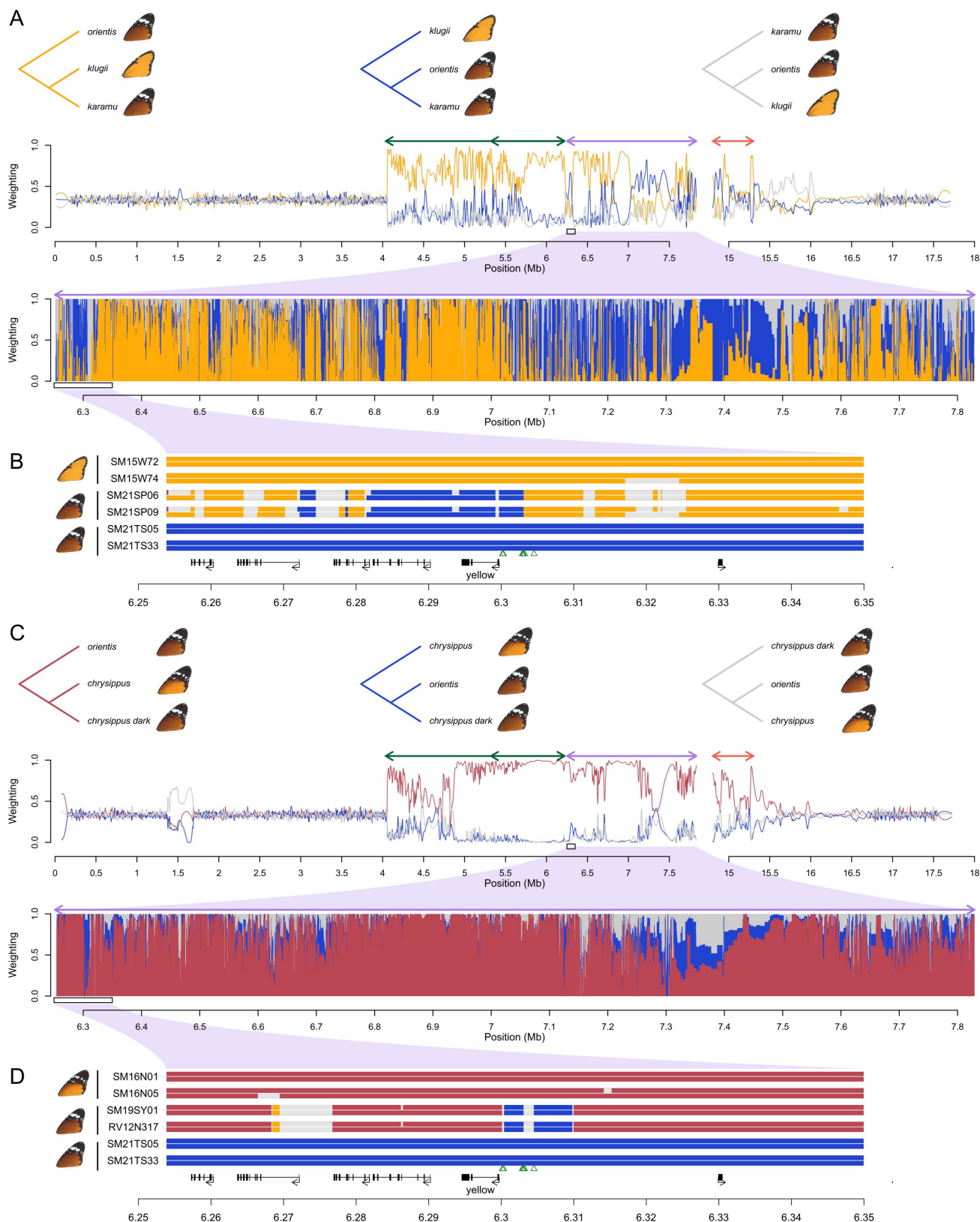
Fig 4. Two independent cases of recombination within the BC supergene with phenotypic consequences. (A) Topology weightings across chr15 showing how the karamu haplotype is related to the klugii and orientis haplotypes. Upper panel shows three possible rooted genealogical topologies.

Second panel shows weights for each topology along the chromosome, smoothed with a 20 kb span. Arrows above the plot indicate the locations of inversions. Third panel shows unsmoothed topology weightings across a 1.5 Mb region corresponding to Inversion 2. (**B**) Ancestry painting from Loter [54] across a 100 kb region within Inversion 2 showing ancestry tracts for two homozygous karamu individuals compared to two representative individuals homozygous for the orientis and klugii haplotypes. Coding regions are indicated below the plot, with the candidate gene for background colouration *yellow* indicated. Green triangles represent the top 10 SNPs for background colour in our GWAS (Fig 1C). There is evidence for recombination throughout the supergene region, and specifically in the vicinity of *yellow*, consistent with the hypothesis that orientis ancestry at this locus (i.e., the *B* allele) is associated with darker colouration in karamu individuals. (**C**, **D**) A second example of recombination in the promoter of *yellow*. Plots are as described for panels A and B, except showing relationships between two individuals from North Africa and Mediterranean with a chrysippus-like haplotype (according to Admixture and ancestry painting), but dark background colouration. Again, orientis ancestry in the promoter region of *yellow* suggests that recombination allowed the transfer of the *B* allele into a different genetic background, causing darker wing colouration. The data underlying this figure can be found in https://doi.org/10.5281/zenodo.14718778.

https://doi.org/10.1371/journal.pbio.3003043.g004

(Fig L in S1 Text). However, there is heterogeneity in these relationships, and occasionally, complete switches to a different relationship within each rearranged region (Fig L in S1 Text). These patterns are consistent with historical gene flux after the inversions occurred.

We next examined patterns of LD between the three pairs of haplotypes. In each case, clear regions of high LD correspond with the previously described rearrangements that differentiate each pair [21] (Fig M in S1 Text). There is also quantitative variation in the extent of LD within inverted tracts, which could be indicative of variation in the extent of gene flux across the chromosomes, but may also reflect other factors such as variation in effective population size. Overall, the generally high LD within inversions, along with high absolute genetic divergence across the length of the supergene (Fig 3), imply that any recent gene flux between these haplotypes has occurred at a low rate.

Finally, we attempted to quantify gene flux between the three major haplotype groups by fitting isolation-with-migration (IM) models, which are conventionally applied to model species divergence with gene flow. Here, haplotype groups are modelled as panmictic populations that became isolated at some point in the past, and gene flux between the distinct haplotype groups is modelled as 'migration' [36]. IM models were fitted using gIMble [57], with separate models for each rearranged region and each pair of haplotype groups, because not all regions are inverted between all pairs. For example, regions 1.1 and 4 are inverted in orientis only, so we expect approximately free recombination between klugii and chrysippus in these regions. Of the eight pairwise tests in which the regions are inverted, three had best-fitting models without gene flux, while the remaining five had estimated effective migration rates (m_e) ranging from 2.42×10^{-11} to 3.09×10^{-6} (this equates to a range of 3.02×10^{-5} to 4.89 effective migrants per generation (M_e) assuming $M_e = m_e 4N_{e\text{ (recipient)}}$; Table 2; Fig N in S1 Text). Higher rates are generally seen between klugii and orientis, but there is no apparent trend with the size of the rearranged region. Of the four tests that involved collinear regions, two had the highest estimated effective migration rates, and two had low or no inferred gene flux. This is probably because these latter two collinear tracts (specifically region 1.2 between chrysippus and orientis, and region 2 between klugii and chrysippus) are nevertheless physically translocated with respect to each other (Fig 3A), probably impairing correct meiotic pairing. Taking these results together, we conclude that there is considerable evidence for history of gene flux in at least some of the rearranged regions of the supergene, but our estimated rates of gene flux should be interpreted with caution given the small size of the regions and resulting sampling noise and reduced inference power (we note that one model failed to optimise), and the modelling restriction of unidirectional gene flux [57].

Discussion

Structural variants that suppress recombination have been found to contribute to local adaptation and the maintenance of complex phenotypic polymorphisms. However, to understand how these variants persist and change over time, it is necessary to go beyond simply

Table 2. Summary of gIMble results highlighting the best fitting models for each region and haplotype pair combination.

Inversion	Pair[1]	Model	Ne pop. A	Ne pop. B	Ne anc.	Div. time	m_e	Composite likelihood
1.1	chrysippus - klugii	IM BA	4.03E+05	4.48E+05	1.76E+06	2.47E+06	3.09E−06	−439547.36
1.1	chrysippus - orientis	DIV	4.02E+05	3.10E+05	1.11E+06	9.30E+05	–	−551959.49
1.1	klugii - orientis	IM BA	5.78E+05	1.34E+05	2.77E+06	4.25E+06	7.20E−07	−605170.81
1.2	chrysippus - klugii	DIV	1.71E+05	1.95E+05	1.05E+06	7.43E+05	–	−283401.45
1.2	chrysippus - orientis	DIV	1.99E+05	2.50E+05	1.11E+06	9.62E+05	–	−321748.64
1.2	klugii - orientis	IM AB	8.00E+04	2.19E+05	1.99E+06	2.27E+06	1.04E−06	−409100.25
2	chrysippus - klugii	IM AB	3.18E+05	2.73E+05	8.76E+05	9.46E+05	3.80E−11	−565003.35
2	chrysippus - orientis	IM AB	3.58E+05	3.12E+05	8.97E+05	9.60E+05	2.42E−11	−596504.91
2	klugii - orientis	DIV	1.97E+05	2.02E+05	8.66E+05	6.67E+05	–	−716365.75
4	chrysippus - klugii	IM AB	3.94E+05	6.43E+05	1.59E+06	2.42E+06	2.71E−06	−399370.26
4	chrysippus - orientis	IM AB	7.10E+05	5.84E+05	1.16E+06	7.62E+05	2.49E−11	−492519.59
4	klugii - orientis	IM BA	7.60E+05	3.14E+05	2.04E+06	3.83E+06	8.79E−07	−493600.45

[1]Populations tested are listed in the order A-B. DIV = divergence with no migration; IM AB = isolation with unidirectional migration from B to A; IM BA = from A to B. Divergence times are in generations.

https://doi.org/10.1371/journal.pbio.3003043.t002

associating genotype and phenotype, and to investigate how sequences evolve within these genomic regions. Here we show that the BC supergene of *D. chrysippus*, which underpins wing colour pattern variation, displays surprising haplotype diversity, with a greater number of divergent haplotype groups than there are described phenotypic morphs. Counterintuitively, this diversity is partly fuelled by recombination. Our findings suggest that supergene evolution is a highly dynamic process, raising a number of further questions.

A paradox of our study is that we report evidence for both historical and recent recombination in a genomic region that was first identified because of its role in suppressing crossing over. In reality, the realised rate of gene flux through recombination in the BC supergene must be low, otherwise we would not have been able to describe the highly diverged haplotype groups, nor to identify recombinants between them. Indeed, although a considerable fraction of our sequenced individuals carry haplotypes showing evidence for recent recombination, many of the recombination breakpoints are shared among individuals, implying that the observed recombinant haplotypes stem from a smaller number of recombination events. Moreover, several recombination points are between adjacent inversions, leaving the inversion haplotypes intact. The modular structure of the supergene means that single crossovers between adjacent inversions can generate modular ancestry mosaics without the production of unbalanced gametes. However, we also observe more complex mosaic ancestries within inversions in some individuals, as well as evidence for long-term gene flux, consistent with some recombination occurring within inversions. A large proportion of this may be attributable to gene conversion, which has been shown to be unimpeded within inversions in *Drosophila* [28–32,38,40]. However, gene conversion cannot easily explain the exchange of long tracts that we observe, such as the 10–20 kb tracts around the *yellow* locus. It is equally difficult to explain these by double crossover events, which should be impeded due to crossover interference in inversions of 1–2 Mb in length. Indeed, chromosome map lengths in the butterflies *Heliconius melpomene* and *Vanessa cardui* average around 50 cm [58,59], implying an average of one crossover per meiosis per bivalent, and in *Leptidea sinapis* only chromosomes >20 Mb (longer than any chromosome in *D. chrysippus*) have map lengths consistent with frequent double crossovers [60]. An alternative explanation for the large tracts of recombinant ancestry within inversions is that these may have been facilitated by recurrent inversion or "toggling" of inversion orientations [61]. Toggling may be common in inversions flanked by segmental

duplications due to recurrent non-allelic homologous recombination (NAHR) events [61], and could serve as a bridge for recombination between inverted haplotypes. Another line of evidence consistent with the toggling hypothesis is a lack of the characteristic "suspension bridge" pattern of divergence reflecting greater recombination suppression near the breakpoints, as seen in some other inversions [35]. Importantly, once a large tract of ancestry has been exchanged (either via double crossover or inversion toggling), the recombined tract is no longer inverted with respect to the haplotype it has invaded. Hence, more complex fine-scale ancestry mosaics such as those we describe can emerge through unrestricted single crossovers in subsequent generations.

Our findings do not provide direct evidence of the potential costs or benefits of recombination within the supergene region. The simplest models of supergene evolution imply that recombinant haplotypes have reduced fitness due to broken associations between co-adapted or locally adapted alleles. It is notable that one particular combination of colour pattern alleles is absent in our data set: haplotypes carrying the *B* (dark) and *C* (absence of forewing tip) alleles. All individuals inferred to be homozygous *BB* based on the best GWAS hit for the B locus (position 6,300,183 on chr15) have a full forewing black tip (implying a *cc* genotype at the C locus). The rarity of the *BC* haplotype in the wild despite its occasional production in breeding experiments has been noted previously [62], and is suggestive of selection against this particular allelic combination. Another intriguing observation is that the population with the highest rate of recent recombinants is the small island of St. Helena, where five of six individuals carry one of two different recombinant haplotypes between chrysippus and orientis. We hypothesise that this population is the result of a recent colonisation bottleneck and that the abundance of recombinant haplotypes may result from relaxed purifying selection. On the other hand, it is also likely that certain recombinant haplotypes are occasionally more fit than the prevailing haplotypes, either because they provide new allelic combinations (including at loci other than B and C) associated with a fit phenotype [5,22,37], or because they allow purging of deleterious mutations [23]. Our finding that several haplotypes with the same complex ancestry mosaics appear in multiple individuals may imply a process of allelic turnover, in which an existing 'allele' (or haplotype group) is in the process of being replaced by a fitter recombinant one. Indeed, the complex pattern of relationships among even the established haplotype groups suggests that recombination and allelic turnover may have occurred repeatedly throughout the evolutionary history of the BC supergene. As a result, it is likely that none of the established haplotype groups we describe here closely resemble the 'original' haplotypes captured when the rearrangements first occurred. A process of dynamic turnover has been suggested in a different supergene system in *Papilio* butterflies [42], and may prove with further work to be the norm for supergenes, as it is for sex chromosomes in some taxa [63].

A puzzling feature of the BC supergene is the apparent long-term persistence of multiple haplotype groups with (apparently) the same phenotypic effects. Specifically, the newly described karamu haplotype found in eastern parts of South Africa is associated with a colour pattern indistinguishable from that of the orientis haplotype found throughout South Africa. Although we initially hypothesised that this may represent a case of ongoing allelic turnover (in which the karamu haplotype may eventually replace the orientis haplotype), this is not supported by the similarly high level of diversity seen in both haplotype groups, implying that neither has experienced a recent or ongoing selective sweep. An alternative explanation is that both of these haplotypes may be adapted to different geographic regions by influencing traits other than colour pattern. It is certainly possible that the BC supergene region, which contains approximately 150 protein-coding genes, contributes to other important ecological traits. Simulations have shown that such adaptations may continue to accumulate after inversions have become established [11]. It is notable that the karamu haplotype appears to have arisen

through recombination between the southern orientis and eastern klugii haplotypes, and appears to be most common in a geographic region intermediate between these two (though our sampling is too sparse to be sure). It is therefore plausible that this haplotype confers an adaptive advantage by combining an optimal warning pattern for southern Africa with other environmental adaptations suited to east Africa. A similar scenario may explain the existence of a dark-coloured morph in North Africa and the Mediterranean with a haplotype that is highly similar to that of the pale-coloured chrysippus morph, but carries orientis-like variants at the promoter of *yellow* that result in dark colouration. In this case, it may be that recombination allowed for allelic replacement at one locus while maintaining the broader locally adapted haplotype. Further investigation into the ecology and fitness of different genotypes and phenotypes is required to test these hypotheses.

Another factor that may shape haplotype diversity is vulnerability of inversions to the accumulation of deleterious mutations. Both theoretical and empirical studies have shown that inversions can accumulate excess deleterious load as a result of their lower effective population size compared to the rest of the genome and their reduced opportunities for recombination [3,23,24]. This may drive turnover if new or recombinant haplotypes have lower mutational load. It has also been suggested that load may promote polymorphism through associative overdominance, in which heterokaryotypes carrying different sets of deleterious recessive alleles have increased fitness relative to homokaryotypes due to masking of the deleterious recessives [23]. While examples of heterokaryotype advantage are known [24], it is difficult to prove that associative overdominance is the cause, especially given that the conditions under which it is likely to evolve are highly restrictive [25]. In *D. chrysippus*, there is no compelling evidence for heterozygote advantage: the three most common haplotype groups each occur in large regions of monomorphism, and broad clines suggest that polymorphism in the hybrid zone reflects a balance between selection (local adaptation) and extensive dispersal [44] rather than heterokaryotype advantage. Further investigation is needed to specifically rule out heterokaryotype advantage, especially for the newly identified karamu haplotype and the other divergent haplotype found north of the Sahara, which are only known from polymorphic locations. It is worth noting that the recent fusion of chr15 (chrysippus haplotype) to the W chromosome in East Africa [45] represents the origin of yet another divergent haplotype that is restricted to the heterozygous state (butterfly females are ZW and do not undergo recombination), and therefore would be sheltered from the effects of deleterious recessives.

The additional divergent haplotype groups described in the present study were identified using only short-read sequencing data, so we cannot confirm whether each of these are also maintained by unique rearrangements of chr15, though this seems highly likely. Using short reads aligned to a single reference also means that insertion, deletion and copy-number variants were not considered, which probably explains our inability to narrow down the C locus. Future work using genome graph approaches will provide an improved understanding of the relationships between structural variation, haplotype diversity and phenotypic variation.

We hypothesise that the unusual physical structure of *Danaus* chromosome 15 has contributed to the emergence of divergent haplotypes. The chromosome carries a large CNV region which began to grow around 7.5 MYA, and now comprises over a third of the chromosome in the klugii haplotype [21]. This region, which is also rich in transposable elements, creates fertile ground for the emergence of new divergent haplotypes through two mechanisms of recombination suppression [21]: It could directly prevent crossing over [64] or indirectly promote recombination suppression by propagating new inversions through NAHR. Whether the physical peculiarities of this chromosome also facilitated its recent fusion to the W chromosome in East Africa remains to be determined. It has been suggested that the occurrence of holocentric chromosomes (centromeres are dispersed across the length of the chromosome) and inverted

meiosis (sister chromatids separate before homologous chromosomes) in the lepidoptera might allow for more rapid evolution of chromosomal rearrangements on average in this insect order [65]. However, a recent analysis of chromosome-scale genomes from 210 lepidopterans revealed that both inter- and intrachromosomal rearrangements are rare overall outside of a few highly rearranged lineages (not including *Danaus*) [66]. The tendency for *Danaus* chromosome 15 to experience rearrangements is therefore more likely a feature of the individual chromosome than of the lineage. This echoes a similar pattern seen in the avian chromosome 4, which has undergone both ancient rearrangements (possibly associated with an ancient supergene [67]), and more recent fusions and further rearrangement in the formation of neo-sex chromosomes [68–70]. It is notable that the *D. Chrysippus* BC supergene, the *Heliconius numata* P supergene [24] and the fire ant social supergene [6] all share the feature of multiple adjacent non-overlapping inversions that appear to share breakpoints. This modular organisation means that crossovers that occur between two inversions are not suppressed, allowing the distinct modules of the supergene to evolve somewhat independently. Modular arrangements may simply be a side effect of 'reuse' of inversion breakpoints (e.g., in repeat-rich regions), but it is plausible that supergenes with this structure may be more likely to persist long-term if it avoids some of the costs of complete recombination suppression.

In conclusion, we have shown that a supergene with an apparently simple phenotypic association shows unexpected diversity at the haplotype level. Our findings bring to light the nuanced relationship between supergenes and recombination, in which incomplete recombination suppression can fuel haplotype diversification, and possibly support long-term persistence. Further work is needed to understand the selective and ecological drivers underlying the observed diversity. Our study adds to a growing body of work revealing the indirect effects of structural variation on the evolution of surrounding sequences [24,36,71,72]. Further work across a diverse range of taxa, along with population genetic modelling will help to uncover the generality of these phenomena.

Methods

Data collection, whole genome sequencing, and genotyping

We produced new whole genome sequence data (Illumina, 150 bp paired-end) from 130 butterflies and combined this with previously sequenced data from additional 44 individuals [21,45,73], resulting in data from 162 wild-caught *D. chrysippus* butterflies representing each of the main colour morphs across Africa and the hybrid zone (Fig 1A and S1 Table) and 12 captively reared individuals. In addition, publicly available sequencing data from one *Danaus melanippus* individual was used in analyses that required an outgroup. Sample collection was conducted with the permission of landowners and under appropriate permits where relevant: Wildlife division of Ghana Forestry Commission: 0174076/024992; National Commission for Science and Technology, Kenya: NACOSTI/P15/3290/3607, NACOSTI/P15/2403/3602; Ministry of Education, Rwanda: MINEDUC/S&T/459/2017; Mpumalanga Parks and Tourism Agency, South Africa: MPB5667; Northern Cape Department of Environment and Nature Conservation, South Africa: FAUNA0615202; Environment and Natural Resources Directorate, St. Helena Government: EMDEP006/17; Council of Fuerteventura, Spain: Permit 604 (2017). All sample information, including accession numbers, are provided in S1 Table.

For samples newly sequenced in this study, the protocol followed our previous work [21]. Briefly, genomic DNA was extracted from ethanol-preserved tissue using the Qiagen DNEasy Blood and Tissue Kit (Qiagen, Redwood City, CA). Illumina library preparation and sequencing (150bp, paired-end) was performed by Novogene (Cambridge, UK), using a Novaseq 6,000 instrument.

Reads were mapped to the Dchry2.2 reference genome (ENA accession GCA_916720795.1; [73]) using BWA mem v0.7.17 [74] with default parameters, and PCR duplicates were removed using PicardTools v2.11.1 (https://broadinstitute.github.io/picard/). Indel realignment was then carried out using GATK v.3.8 [75]. To identify any substantial variation in read depth across the dataset, mean read depth was calculated using Mosdepth [76]. One individual was found to have substantially higher read depth (SM18W01) and as a result the bam file for this individual was randomly downsampled to 30% of its original size using SAMtools ([77]; samtools view -s 0.30) to eliminate biases in genotyping. Genotyping was carried out using BCFtools [78], with genotypes on the Z chromosome (chr1) called by defining ploidy based on known sex (i.e., females as haploid and males as diploid). Genotypes were then filtered using BCFtools to remove any positions called fewer than twice and to leave only genotypes with an individual depth of ≥7 and with genotype quality of ≥30. Additional filtering to remove SNPs with >10% missing data (corresponding to a haploid count of 313 across autosomes and 224 on the Z chromosome), was performed for most remaining analyses, except when otherwise specified.

Population structure, diversity, and divergence

Genomic variation across our dataset, spanning different regions of the genome, was assessed by producing PCAs from different sets of SNPs using PLINK [79]. Two SNP sets were used, representing (i) the autosomal regions of the genome excluding chr15 as well as the Z sex chromosome chr1 (14,548,985 SNPs), and (ii) rearranged regions 1, 2, and 4 of the BC supergene on chr15, described in [21] (173,998 SNPs). Genome-wide nucleotide diversity (π), F_{ST}, and d_{XY} were computed in non-overlapping 50 kb windows across the genome using the script *popgenWindows.py* (github.com/simonhmartin/genomics_general release 0.5) and

netdivergence (d_a) was calculated from this output (calculated as $d_a = d_{XY} - \dfrac{\left(\pi_{P1} + \pi_{P2}\right)}{2}$ where

P1 and P2 represent Population 1 and Population 2, respectively), following equations 10.5 for π, 10.20 for d_{XY}, and 10.21 for d_a in Nei [80]. For each pair of haplotypes compared, only sites that had non-missing genotypes in both haplotypes were considered when computing the proportion of differences.

Genome-wide association

The association between SNP variation and phenotypic variation was analysed using a GWAS analysis implemented in PLINK across all chromosomes. Phenotypes of scanned wings from 172 individuals were scored following [44] based on whether the background colour was pale (1), intermediate (2), or dark (3), and whether the forewing band was absent (1), partial (2), or present (3) (wings were not available to phenotype for two individuals resulting in their omission from the GWAS). Empirical *p*-values were computed using the default adaptive permutation method implemented in PLINK. To confirm that geographic sampling structure alone does not underpin the patterns of association observed across the genome we re-ran the GWAS using only the 87 individuals from the hybrid zone for which we had phenotypes (populations NYA, NRB, and MPL).

Visualising variation in the BC supergene using Neighbor-Net

To visualise genetic relationships and clustering across the BC supergene, we generated a phylogenetic network based on pairwise genetic distances among diploid individuals using the Neighbor-Net algorithm [81], implemented in SplitsTree [82]. Pairwise distances were computed using the script distMat.py (github.com/simonhmartin/genomics_general release 0.5),

which computes the average pairwise distance between the four pairs of sequence haplotypes for each pair of diploid individuals. This analysis was computed using modules 1, 2, and 4 of the supergene region [21]. Input genotypes were filtered using the script filterGenotypes.py (github.com/simonhmartin/genomics_general release 0.5) to retain sites where at least 50% of individuals had non-missing data (after depth and quality filtering described above), where fewer than 75% of individuals were heterozygous, and where the minor allele was present at least twice.

Admixture

We aimed to naively determine the number of distinct haplotype groups of the supergene by modelling each individual in terms of its ancestry from a fixed number of source populations. To this end, we ran Admixture v1.3.0 [53] on a concatenated dataset of loci from across the supergene modules 1, 2, and 4 (i.e., excluding the CNV region). Admixture was run specifying a range of clusters from $k = 3$ to $k = 12$ (Fig D in S1 Text) and 20-fold cross-validation error ($--cv = 20$) was computed.

Phasing

Phasing was carried out to assist with ancestry painting using two consecutive tools, Whatshap v1.1 [83], a read-based phasing software, and Shapeit4 v4.2.2 [84] a statistical phasing software using default parameters.

Ancestry painting and additional phase correction

To visualise genetic clustering of phased haplotypes, we used two approaches for ancestry painting along the chromosome. Both approaches require defined reference individuals, which were selected based on the Admixture analysis above. Reference individuals used for each analysis are described in the Results.

The first approach was Loter [54], which uses a hidden Markov model to assign ancestry and identify breakpoints along the genome. First, phased genotypes were filtered using filterGenotypes.py (github.com/simonhmartin/genomics_general release 0.5) to remove any sites at which more than 60% of individuals are heterozygous, as such sites are likely to be caused by mis-mapping and could be prone to break tracts of ancestry. Haploid genotypes were output as counts of the minor allele (0 or 1), and Loter was run using the python API in a wrapper script (loter_wrapper.py), with options rate_vote = 0, nb_bagging = 20. Adjacent SNPs with identical ancestry scores were concatenated into tracts to reduce the output file size.

A second approach for ancestry painting that we call 'distPaint' was applied to confirm the Loter results, while providing a coarser visualisation at the whole-chromosome scale. This approach uses a sliding-window along the genome and assigns ancestry for each haplotype based on genetic distance (d_{XY}) from the reference sets of individuals. A window size of 200 SNPs was used. Ancestry was assigned if this difference was significantly lower for one reference population according to a Wilcoxon Rank Sum test ($p \leq 0.01$), otherwise ancestry was set to undefined. This was implemented using a custom python script distPaint.py (github.com/simonhmartin/genomics_general release 0.5).

Initial visualisation of the ancestry painting from both approaches revealed obvious cases of phasing errors (Fig K in S1 Text). Such errors could lead to false-positive inference of recombination events. For example, say an individual is phased into two haplotypes, that are then painted with ancestries "c-c-c-c-k" and "k-k-k-k-c" (where c and k represent tracts of chromosome assigned to reference populations chrysippus and klugii, respectively). This

could either represent a case of an individual carrying two recombinant haplotypes in which both recombination events happened to occur at the same genomic region, or it could be a case of a single phasing error in an individual that in fact caries two common haplotypes (c-c-c-c-c and k-k-k-k-k). The latter is of course far more likely. We therefore applied a final heuristic phase correction approach to the inferred ancestries which attempts to maximise similarity among haplotypes at the whole-chromosome scale, thereby minimising inferred recombination events (Fig K in S1 Text). For each diploid individual, this heuristic approach iterates over each ancestry-painted tract in the chromosome (e.g., from Loter) and switches the phase if this would cause an increase in similarity of the two resulting haplotypes to one or more other haplotypes in the full dataset (considering all ancestry blocks up to and including the focal one). Because we are interested in identifying common shared haplotypes, we consider the average similarity of the top three most similar haplotypes in the rest of the dataset. The process is performed left-to-right and then right-to-left for each individual, and then repeated again starting from the first individual, up to a total of 20 iterations for Loter outputs and 500 iterations for distPaint.py outputs (the latter have fewer intervals, allowing for more rapid computation). This algorithm is implemented in the script phasepaint.py (https://github.com/simonhmartin/phasepaint release 0.1).

Topology weighting

To complement the ancestry painting described above, we analysed changes in relationships among supergene haplotypes across the chromosome (as an indicator of possible recombination), using topology weighting [56], implemented in TWISST2 (https://github.com/simonhmartin/twisst2 release 0.0.3). This approach infers genealogies and where they change along the genome, and outputs a 'weighting' for each possible topology for the relationships between defined groups of individuals in each genomic region. Input genotypes were filtered using the script filterGenotypes.py (github.com/simonhmartin/genomics_general release 0.5) to retain sites where at least 50% of individuals had non-missing data (after depth and quality filtering described above), where fewer than 75% of individuals were heterozygous, and where the minor allele was present at least twice. An outgroup was needed for polarisation, for which we used a single *D. melanippus* individual (S1 Table), following the alignment and genotyping procedures described above.

Linkage disequilibrium analysis

LD between pairs of sites across chromosome 15 was quantified using the r^2 metric, computed using PLINK [79] with the flag --r2. The computation was run first on all 174 individuals, and then on three subsets representing each pair of reference individuals for chrysippus (population NGA), klugii (WAT) and orientis (TSW). SNPs with a minor allele frequency <0.2 were excluded, as were all SNPs within the CNV region. Finally, SNPs were thinned randomly to retain ~20,000 for each comparison. LD heatmaps were plotted using the LDheatmap package [85] in R.

Modelling gene flux using gIMble

To detect and quantify gene flux between supergene haplotypes, we fitted IM models for individuals homozygous for the chrysippus, klugii, orientis alleles using the gIMble framework [57]. Under the IM model, gene-flux between supergene haplotypes is modelled as migration (gene flow) between panmictic populations. Six klugii individuals (WAT population), seven orientis individuals (TSW population), and six chrysippus (NGA population) were included in the analysis (S1 Table). Since gIMble carries out pairwise tests this resulted in six pairwise

tests for each of the four regions tested. A VCF containing only data from these 19 individuals was first preprocessed using *gimble preprocess*. Next, intergenic bed files were produced by using bedtools intersect and bedtools subtract to extract and then exclude genic regions using the reference annotation file. *gimble parse* was then run for each combination of supergene region (i.e., regions 1.1, 1.2, 2, and 4, Fig 3A) and pairwise comparison, followed by *gimble blocks*, *gimble windows*, *gimble info*, and *gimble tally*. *gimble optimize* was then run for each combination of region and pairwise test specifying each of three models, DIV—a divergence only model, IM_AB an IM model where gene flow occurs from population B into A, and IM_BA an IM model where gene flow occurs from population A into B, resulting in a total of 36 models. *gimble query* was then run to extract model summary information, including composite likelihood, for each model allowing us to determine the best fitting of the three models for each of the 12 region and pair combinations (full results are reported in S2 Table. For detailed commands and model parameters see archived GitHub repository: https://doi.org/10.5281/zenodo.14726309.

Supporting information

S1 Text. Figures A–N.
(PDF)

S1 Table. Sample information for all 174 *Danaus chrysippus* individuals and one outgroup *Danaus melanippus*, including sampling location, sex, phenotypes, and read accessions.
(XLSX)

S2 Table. Full results of gIMble analyses.
(XLSX)

Acknowledgments

We thank the following people for assistance with sampling, breeding and acquisition of permissions: Rwanda—Constantin Sibomana and Jody Garbe; Kenya—Piera Ireri, Ivy Ng'Iru, Godfrey Etelej, David Smith, Anna Orteu, Jenny York, Owen McMillan, Valarie McMillan; South Africa—Jeremy Dobson; Ghana—Oskar Brattstrom; Spain (Fuerteventura) —Yeray Monasterio, David Smith; Tunisia—Roger Vila; Italy—Richard ffrench-Constant; St. Helena—David Pryce. We also thank Brian Charlesworth, Deborah Charlesworth, David Smith, Richard ffrench-Constant, Chay Graham, Thomas Decroly, Alexander Mackintosh, Domink Laetsch and Konrad Lohse for valuable input on this work.

Author contributions

Conceptualisation: Rishi De-Kayne, Ian J. Gordon, Simon H. Martin.

Data curation: Rishi De-Kayne, Simon H. Martin.

Formal analysis: Rishi De-Kayne, Simon H. Martin.

Funding acquisition: Ian J. Gordon, Simon H. Martin.

Investigation: Rishi De-Kayne, Ian J. Gordon, Reinier F. Terblanche, Kennedy Saitoti Omufwoko, Simon H. Martin.

Methodology: Rishi De-Kayne, Ian J. Gordon, Simon H. Martin.

Project administration: Ian J. Gordon, Reinier F. Terblanche, Steve Collins, Dino J. Martins, Simon H. Martin.

Resources: Ian J. Gordon, Steve Collins, Dino J. Martins, Simon H. Martin.

Software: Rishi De-Kayne, Simon H. Martin.

Supervision: Simon H. Martin.

Validation: Rishi De-Kayne.

Visualisation: Rishi De-Kayne, Simon H. Martin.

Writing – original draft: Rishi De-Kayne, Simon H. Martin.

Writing – review & editing: Rishi De-Kayne, Simon H. Martin.

References

1. Charlesworth B, Charlesworth D. Selection of new inversions in multi-locus genetic systems. Genet Res. 1973;21:167–83.

2. Thompson MJ, Jiggins CD. Supergenes and their role in evolution. Heredity (Edinb). 2014;113(1):1–8. https://doi.org/10.1038/hdy.2014.20 PMID: 24642887

3. Charlesworth B. The effects of inversion polymorphisms on patterns of neutral genetic diversity. Genetics. 2023;224(4):iyad116. https://doi.org/10.1093/genetics/iyad116 PMID: 37348059

4. Mérot C, Llaurens V, Normandeau E, Bernatchez L, Wellenreuther M. Balancing selection via life-history trade-offs maintains an inversion polymorphism in a seaweed fly. Nat Commun. 2020;11:670.

5. Küpper C, Stocks M, Risse JE, Dos Remedios N, Farrell LL, McRae SB, et al. A supergene determines highly divergent male reproductive morphs in the ruff. Nat Genet. 2016;48(1):79–83. https://doi.org/10.1038/ng.3443 PMID: 26569125

6. Yan Z, Martin SH, Gotzek D, Arsenault SV, Duchen P, Helleu Q, et al. Evolution of a supergene that regulates a trans-species social polymorphism. Nat Ecol Evol. 2020;4:240–9.

7. Li J, Cocker JM, Wright J, Webster MA, McMullan M, Dyer S, et al. Genetic architecture and evolution of the S locus supergene in Primula vulgaris. Nat Plants. 2016;2(12):16188. https://doi.org/10.1038/nplants.2016.188 PMID: 27909301

8. Kim K-W, Bennison C, Hemmings N, Brookes L, Hurley LL, Griffith SC, et al. A sex-linked supergene controls sperm morphology and swimming speed in a songbird. Nat Ecol Evol. 2017;1(8):1168–76. https://doi.org/10.1038/s41559-017-0235-2 PMID: 29046578

9. Komata S, Kajitani R, Itoh T, Fujiwara H. Genomic architecture and functional unit of mimicry supergene in female limited Batesian mimic Papilio butterflies. Philos Trans R Soc Lond B Biol Sci. 2022;377:20210198. https://doi.org/10.1098/rstb.2021.0198

10. Kirkpatrick M, Barton N. Chromosome inversions, local adaptation and speciation. Genetics. 2006;173(1):419–34. https://doi.org/10.1534/genetics.105.047985 PMID: 16204214

11. Schaal SM, Haller BC, Lotterhos KE. Inversion invasions: when the genetic basis of local adaptation is concentrated within inversions in the face of gene flow. Philos Trans R Soc Lond B Biol Sci. 2022;377:20210200.

12. Berdan EL, Barton NH, Butlin R, Charlesworth B, Faria R, Fragata I. How chromosomal inversions reorient the evolutionary process. J Evol Biol. 2023;36:1761–82.

13. Lowry DB, Willis JH. A widespread chromosomal inversion polymorphism contributes to a major life-history transition, local adaptation, and reproductive isolation. PLoS Biol. 2010;8(9):e1000500. https://doi.org/10.1371/journal.pbio.1000500 PMID: 20927411

14. Hager ER, Harringmeyer OS, Wooldridge TB, Theingi S, Gable JT, McFadden S, et al. A chromosomal inversion contributes to divergence in multiple traits between deer mouse ecotypes. Science. 2022;377(6604):399–405. https://doi.org/10.1126/science.abg0718 PMID: 35862520

15. Huang K, Andrew RL, Owens GL, Ostevik KL, Rieseberg LH. Multiple chromosomal inversions contribute to adaptive divergence of a dune sunflower ecotype. Mol Ecol. 2020;29(14):2535–49. https://doi.org/10.1111/mec.15428 PMID: 32246540

16. Kapun M, Fabian DK, Goudet J, Flatt T. Genomic evidence for adaptive inversion clines in Drosophila melanogaster. Mol Biol Evol. 2016;33(5):1317–36. https://doi.org/10.1093/molbev/msw016 PMID: 26796550

17. Todesco M, Owens GL, Bercovich N, Légaré J-S, Soudi S, Burge DO, et al. Massive haplotypes underlie ecotypic differentiation in sunflowers. Nature. 2020;584(7822):602–7. https://doi.org/10.1038/s41586-020-2467-6 PMID: 32641831

18. Harringmeyer OS, Hoekstra HE. Chromosomal inversion polymorphisms shape the genomic landscape of deer mice. Nat Ecol Evol. 2022;6(12):1965–79. https://doi.org/10.1038/s41559-022-01890-0 PMID: 36253543

19. Morales HE, Faria R, Johannesson K, Larsson T, Panova M, Westram AM, et al. Genomic architecture of parallel ecological divergence: Beyond a single environmental contrast. Sci Adv. 2019;5(12):eaav9963. https://doi.org/10.1126/sciadv.aav9963 PMID: 31840052

20. Joron M, Frezal L, Jones RT, Chamberlain NL, Lee SF, Haag CR, et al. Chromosomal rearrangements maintain a polymorphic supergene controlling butterfly mimicry. Nature. 2011;477(7363):203–6. https://doi.org/10.1038/nature10341 PMID: 21841803

21. Kim K-W, De-Kayne R, Gordon IJ, Omufwoko KS, Martins DJ, Ffrench-Constant R, et al. Stepwise evolution of a butterfly supergene via duplication and inversion. Philos Trans R Soc Lond B Biol Sci. 2022;377(1856):20210207. https://doi.org/10.1098/rstb.2021.0207 PMID: 35694743

22. Roesti M, Gilbert KJ, Samuk K. Chromosomal inversions can limit adaptation to new environments. Mol Ecol. 2022;31:4435–9.

23. Berdan EL, Blanckaert A, Butlin RK, Bank C. Deleterious mutation accumulation and the long-term fate of chromosomal inversions. PLoS Genet. 2021;17(3):e1009411. https://doi.org/10.1371/journal.pgen.1009411 PMID: 33661924

24. Jay P, Chouteau M, Whibley A, Bastide H, Parrinello H, Llaurens V, et al. Mutation load at a mimicry supergene sheds new light on the evolution of inversion polymorphisms. Nat Genet. 2021;53(3):288–93. https://doi.org/10.1038/s41588-020-00771-1 PMID: 33495598

25. Charlesworth B. The fitness consequences of genetic divergence between polymorphic gene arrangements. Genetics. 2024;226(3):iyad218. https://doi.org/10.1093/genetics/iyad218 PMID: 38147527

26. Jay P, Aubier TG, Joron M. The interplay of local adaptation and gene flow may lead to the formation of supergenes. Mol Ecol. 2024:e17297.

27. Sturtevant AH, Beadle GW. The relations of inversions in the X chromosome of *Drosophila melanogaster* to crossing over and disjunction. Genetics. 1936;21(5):554–604. https://doi.org/10.1093/genetics/21.5.554 PMID: 17246812

28. Navarro A, Betrán E, Barbadilla A, Ruiz A. Recombination and gene flux caused by gene conversion and crossing over in inversion heterokaryotypes. Genetics. 1997;146(2):695–709. https://doi.org/10.1093/genetics/146.2.695 PMID: 9178017

29. Chovnick A. Gene conversion and transfer of genetic information within the inverted region of inversion heterozygotes. Genetics. 1973;75(1):123–31. https://doi.org/10.1093/genetics/75.1.123 PMID: 4202769

30. Crown KN, Miller DE, Sekelsky J, Hawley RS. Local inversion heterozygosity alters recombination throughout the genome. Curr Biol. 2018;28(18):2984–90.e3. https://doi.org/10.1016/j.cub.2018.07.004 PMID: 30174188

31. Korunes KL, Noor MAF. Pervasive gene conversion in chromosomal inversion heterozygotes. Mol Ecol. 2019;28(6):1302–15. https://doi.org/10.1111/mec.14921 PMID: 30387889

32. Schaeffer SW, Anderson WW. Mechanisms of genetic exchange within the chromosomal inversions of *Drosophila pseudoobscura*. Genetics. 2005;171(4):1729–39. https://doi.org/10.1534/genetics.105.041947 PMID: 16143625

33. Rozas J, Aguadé M. Transfer of genetic information in the rp49 region of *Drosophila subobscura* between different chromosomal gene arrangements. Proc Natl Acad Sci U S A. 1993;90(17):8083–7. https://doi.org/10.1073/pnas.90.17.8083 PMID: 8367467

34. Corbett-Detig RB, Hartl DL. Population genomics of inversion polymorphisms in *Drosophila melanogaster*. PLoS Genet. 2012;8(12):e1003056. https://doi.org/10.1371/journal.pgen.1003056 PMID: 23284285

35. Kapun M, Mitchell ED, Kawecki TJ, Schmidt P, Flatt T. An ancestral balanced inversion polymorphism confers global adaptation. Mol Biol Evol. 2023;40(6):msad118. https://doi.org/10.1093/molbev/msad118 PMID: 37220650

36. Lundberg M, Mackintosh A, Petri A, Bensch S. Inversions maintain differences between migratory phenotypes of a songbird. Nat Commun. 2023;14(1):452. https://doi.org/10.1038/s41467-023-36167-y PMID: 36707538

37. Hill J, Enbody ED, Bi H, Lamichhaney S, Lei W, Chen J, et al. Low mutation load in a supergene underpinning alternative male mating strategies in ruff (*Calidris pugnax*). Mol Biol Evol. 2023;40(12):msad224. https://doi.org/10.1093/molbev/msad224 PMID: 37804117

38. Rozas J, Aguadé M. Gene conversion is involved in the transfer of genetic information between naturally occurring inversions of *Drosophila*. Proc Natl Acad Sci U S A. 1994;91(24):11517–21. https://doi.org/10.1073/pnas.91.24.11517 PMID: 7972094

39. Betrán E, Rozas J, Navarro A, Barbadilla A. The estimation of the number and the length distribution of gene conversion tracts from population DNA sequence data. Genetics. 1997;146(1):89–99. https://doi.org/10.1093/genetics/146.1.89 PMID: 9136003

40. Schaeffer SW, Richards S, Fuller Z. Genomics of natural populations: gene conversion events reveal selected genes within the inversions of *Drosophila pseudoobscura*. G3 (Bethesda). 2024;14:jkae176.

41. Fuller ZL, Haynes GD, Richards S, Schaeffer SW. Genomics of natural populations: evolutionary forces that establish and maintain gene arrangements in *Drosophila pseudoobscura*. Mol Ecol. 2017;26(23):6539–62. https://doi.org/10.1111/mec.14381 PMID: 29055159

42. Palmer DH, Kronforst MR. A shared genetic basis of mimicry across swallowtail butterflies points to ancestral co-option of doublesex. Nat Commun. 2020;11(1):6. https://doi.org/10.1038/s41467-019-13859-y PMID: 31900419

43. Smith D, Owen D, Gordon I, Lowis N. The butterfly *Danaus chrysippus* (L.) in East Africa: polymorphism and morph-ratio clines within a complex, extensive and dynamic hybrid zone. Zool J Linn Soc. 1997;120:51–78.

44. Liu W, Smith DAS, Raina G, Stanforth R, Ng'Iru I, Ireri P, et al. Global biogeography of warning coloration in the butterfly *Danaus chrysippus*. Biol Lett. 2022;18(6):20210639. https://doi.org/10.1098/rsbl.2021.0639 PMID: 35642381

45. Martin SH, Singh KS, Gordon IJ, Omufwoko KS, Collins S, Warren IA, et al. Whole-chromosome hitchhiking driven by a male-killing endosymbiont. PLoS Biol. 2020;18(2):e3000610. https://doi.org/10.1371/journal.pbio.3000610 PMID: 32108180

46. Clarke CA, Sheppard PM, Smith AG. genetics of fore and hindwing color in crosses between *Danaus chrysippus* from Australia and from Sierra Leone (Danaidae). Lepidopterists Soc J. 1973.

47. Smith DAS. Genetics of some polymorphic forms of the African butterfly *Danaus chrysippus* L. (Lepidoptera: Danaidae). Insect Syst Evol. 1975;6(2):134–44. https://doi.org/10.1163/187631275x00235

48. Smith DAS, Gordon IJ, Allen JA. Reinforcement in hybrids among once isolated semispecies of *Danaus chrysippus* (L.) and evidence for sex chromosome evolution. Ecol Entomol. 2010;35:77–89.

49. Smith DAS, Gordon IJ, Traut W, Herren J, Collins S, Martins DJ, et al. A neo-W chromosome in a tropical butterfly links colour pattern, male-killing, and speciation. Proc Biol Sci. 2016;283(1835):20160821. https://doi.org/10.1098/rspb.2016.0821 PMID: 27440667

50. Smith DA. Evidence for autosomal meiotic drive in the butterfly *Danaus chrysippus* L. Heredity (Edinb). 1976;36(1):139–42. https://doi.org/10.1038/hdy.1976.13 PMID: 1062366

51. Wittkopp PJ, Vaccaro K, Carroll SB. Evolution of yellow gene regulation and pigmentation in *Drosophila*. Curr Biol. 2002;12(18):1547–56. https://doi.org/10.1016/s0960-9822(02)01113-2 PMID: 12372246

52. Galant R, Skeath JB, Paddock S, Lewis DL, Carroll SB. Expression pattern of a butterfly achaete-scute homolog reveals the homology of butterfly wing scales and insect sensory bristles. Curr Biol. 1998;8(14):807–13. https://doi.org/10.1016/s0960-9822(98)70322-7 PMID: 9663389

53. Alexander DH, Lange K. Enhancements to the ADMIXTURE algorithm for individual ancestry estimation. BMC Bioinformatics. 2011;12:246. https://doi.org/10.1186/1471-2105-12-246 PMID: 21682921

54. Dias-Alves T, Mairal J, Blum MGB. Loter: a software package to infer local ancestry for a wide range of species. Mol Biol Evol. 2018;35(9):2318–26. https://doi.org/10.1093/molbev/msy126 PMID: 29931083

55. Chen J-M, Cooper DN, Chuzhanova N, Férec C, Patrinos GP. Gene conversion: mechanisms, evolution and human disease. Nat Rev Genet. 2007;8(10):762–75. https://doi.org/10.1038/nrg2193 PMID: 17846636

56. Martin SH, Van Belleghem SM. Exploring evolutionary relationships across the genome using topology weighting. Genetics. 2017;206(1):429–38. https://doi.org/10.1534/genetics.116.194720 PMID: 28341652

57. Laetsch DR, Bisschop G, Martin SH, Aeschbacher S, Setter D, Lohse K. Demographically explicit scans for barriers to gene flow using gIMble. PLoS Genet. 2023;19(10):e1010999. https://doi.org/10.1371/journal.pgen.1010999 PMID: 37816069

58. Davey JW, Chouteau M, Barker SL, Maroja L, Baxter SW, Simpson F, et al. Major improvements to the *Heliconius melpomene* genome assembly used to confirm 10 chromosome fusion events in 6 million years of butterfly evolution. G3 (Bethesda). 2016;6(3):695–708. https://doi.org/10.1534/g3.115.023655 PMID: 26772750

59. Shipilina D, Näsvall K, Höök L, Vila R, Talavera G, Backström N. Linkage mapping and genome annotation give novel insights into gene family expansions and regional recombination rate variation in the painted lady (*Vanessa cardui*) butterfly. Genomics. 2022;114(6):110481. https://doi.org/10.1016/j.ygeno.2022.110481 PMID: 36115505

60. Näsvall K, Boman J, Höök L, Vila R, Wiklund C, Backström N. Nascent evolution of recombination rate differences as a consequence of chromosomal rearrangements. PLoS Genet. 2023;19(8):e1010717. https://doi.org/10.1371/journal.pgen.1010717 PMID: 37549188

61. Porubsky D, Sanders AD, Höps W, Hsieh P, Sulovari A, Li R, et al. Recurrent inversion toggling and great ape genome evolution. Nat Genet. 2020;52(8):849–58. https://doi.org/10.1038/s41588-020-0646-x PMID: 32541924

62. Smith D. Heterosis, epistasis and linkage disequilibrium in a wild population of the polymorphic butterfly *Danaus chrysippus* (L.). Zool J Linn Soc. 1980;69:87–109.

63. Vicoso B. Molecular and evolutionary dynamics of animal sex-chromosome turnover. Nat Ecol Evol. 2019;3:1632–41.

64. Huang Y, Gao Y, Ly K, Lin L, Lambooij JP, King EG, et al. Varying recombination landscapes between individuals are driven by polymorphic transposable elements. bioRxiv. 2024. https://doi.org/10.1101/2024.09.17.613564 PMID: 39345575

65. Lukhtanov VA, Dincă V, Friberg M, Šíchová J, Olofsson M, Vila R, et al. Versatility of multivalent orientation, inverted meiosis, and rescued fitness in holocentric chromosomal hybrids. Proc Natl Acad Sci U S A. 2018;115(41):E9610–9. https://doi.org/10.1073/pnas.1802610115 PMID: 30266792

66. Wright CJ, Stevens L, Mackintosh A, Lawniczak M, Blaxter M. Comparative genomics reveals the dynamics of chromosome evolution in Lepidoptera. Nat Ecol Evol. 2024;8(4):777–90. https://doi.org/10.1038/s41559-024-02329-4 PMID: 38383850

67. Mirarab S, Rivas-González I, Feng S, Stiller J, Fang Q, Mai U, et al. A region of suppressed recombination misleads neoavian phylogenomics. Proc Natl Acad Sci U S A. 2024;121(15):e2319506121. https://doi.org/10.1073/pnas.2319506121 PMID: 38557186

68. Sigeman H, Strandh M, Proux-Wéra E, Kutschera VE, Ponnikas S, Zhang H, et al. Avian neo-sex chromosomes reveal dynamics of recombination suppression and W degeneration. Mol Biol Evol. 2021;38:5275–91.

69. Sigeman H, Zhang H, Ali Abed S, Hansson B. A novel neo-sex chromosome in *Sylvietta brachyura* (Macrosphenidae) adds to the extraordinary avian sex chromosome diversity among Sylvioidea songbirds. J Evol Biol. 2022;35(12):1797–805. https://doi.org/10.1111/jeb.14096 PMID: 36156325

70. Dierickx EG, Sin SYW, van Veelen HPJ, Brooke M de L, Liu Y, Edwards SV, et al. Genetic diversity, demographic history and neo-sex chromosomes in the Critically Endangered Raso lark. Proc Biol Sci. 2020;287(1922):20192613. https://doi.org/10.1098/rspb.2019.2613 PMID: 32126957

71. Huang K, Ostevik KL, Elphinstone C, Todesco M, Bercovich N, Owens GL, et al. Mutation load in sunflower inversions is negatively correlated with inversion heterozygosity. Mol Biol Evol. 2022;39(5):msac101. https://doi.org/10.1093/molbev/msac101 PMID: 35535689

72. Jeong H, Baran NM, Sun D, Chatterjee P, Layman TS, Balakrishnan CN, et al. Dynamic molecular evolution of a supergene with suppressed recombination in white-throated sparrows. Elife. 2022;11:e79387. https://doi.org/10.7554/eLife.79387 PMID: 36040313

73. Singh KS, De-Kayne R, Omufwoko KS, Martins DJ, Bass C, Ffrench-Constant R, et al. Genome assembly of *Danaus chrysippus* and comparison with the Monarch *Danaus plexippus*. G3 (Bethesda). 2022;12(3):jkab449. https://doi.org/10.1093/g3journal/jkab449 PMID: 35100331

74. Li H, Durbin R. Fast and accurate long-read alignment with Burrows-Wheeler transform. Bioinformatics. 2010;26(5):589–95. https://doi.org/10.1093/bioinformatics/btp698 PMID: 20080505

75. Poplin R, Ruano-Rubio V, DePristo MA, Fennell TJ, Carneiro MO, der Auwera GAV, et al. Scaling accurate genetic variant discovery to tens of thousands of samples. bioRxiv. 2017;201178.

76. Pedersen BS, Quinlan AR. Mosdepth: quick coverage calculation for genomes and exomes. Bioinformatics. 2018;34(5):867–8. https://doi.org/10.1093/bioinformatics/btx699 PMID: 29096012

77. Li H, Handsaker B, Wysoker A, Fennell T, Ruan J, Homer N, et al. The sequence alignment/map format and SAMtools. Bioinformatics. 2009;25(16):2078–9. https://doi.org/10.1093/bioinformatics/btp352 PMID: 19505943

78. Danecek P, Bonfield JK, Liddle J, Marshall J, Ohan V, Pollard MO, et al. Twelve years of SAMtools and BCFtools. Gigascience. 2021;10(2):giab008. https://doi.org/10.1093/gigascience/giab008 PMID: 33590861

79. Purcell S, Neale B, Todd-Brown K, Thomas L, Ferreira MAR, Bender D, et al. PLINK: a tool set for whole-genome association and population-based linkage analyses. Am J Hum Genet. 2007;81(3):559–75. https://doi.org/10.1086/519795 PMID: 17701901

80. Nei M. Molecular evolutionary genetics. New York, Chichester, West Sussex: Columbia University Press; 1987. p. 433–96.

81. Bryant D, Moulton V. Neighbor-net: an agglomerative method for the construction of phylogenetic networks. Mol Biol Evol. 2004;21(2):255–65. https://doi.org/10.1093/molbev/msh018 PMID: 14660700

82. Huson DH, Bryant D. Application of phylogenetic networks in evolutionary studies. Mol Biol Evol. 2006;23(2):254–67. https://doi.org/10.1093/molbev/msj030 PMID: 16221896

83. Martin M, Patterson M, Garg S, Fischer SO, Pisanti N, Klau GW, et al. WhatsHap: fast and accurate read-based phasing. bioRxiv. 2016:085050. https://doi.org/10.1101/085050

84. Delaneau O, Zagury J-F, Robinson M, Marchini J, Dermitzakis E. Accurate, scalable and integrative haplotype estimation. Nat Commun. 2019;10:5436. https://doi.org/10.1038/s41467-019-13256-1

85. Shin J-H, Blay S, Graham J, McNeney B. LDheatmap: an R function for graphical display of pairwise linkage disequilibria between single nucleotide polymorphisms. J Stat Softw. 2006;16(1):1–9.